Title

Identification of secretory autophagy as a mechanism modulating activity-induced synaptic remodeling.

Journal

Proceedings of the National Academy of Sciences, 121(16)

Authors

Chang, Yen-Ching
Gao, Yuan
Lee, Joo Yeun
et al.

Publication Date

2024-04-16

DOI

10.1073/pnas.2315958121

Peer reviewed

PNAS RESEARCH ARTICLE | GENETICS

Identification of secretory autophagy as a mechanism modulating activity-induced synaptic remodeling

Yen-Ching Chang[a,1], Yuan Gao[a,1], Joo Yeun Lee[a,2], Yi-Jheng Peng[a], Jennifer Langen[a,3], and Karen T. Chang[a,b,4]

Edited by Hugo Bellen, Baylor College of Medicine, Houston, TX; received September 14, 2023; accepted February 23, 2024

The ability of neurons to rapidly remodel their synaptic structure and strength in response to neuronal activity is highly conserved across species and crucial for complex brain functions. However, mechanisms required to elicit and coordinate the acute, activity-dependent structural changes across synapses are not well understood, as neurodevelopment and structural plasticity are tightly linked. Here, using an RNAi screen in *Drosophila* against genes affecting nervous system functions in humans, we uncouple cellular processes important for synaptic plasticity and synapse development. We find mutations associated with neurodegenerative and mental health disorders are 2-times more likely to affect activity-induced synaptic remodeling than synapse development. We report that while both synapse development and activity-induced synaptic remodeling at the fly NMJ require macroautophagy (hereafter referred to as autophagy), bifurcation in the autophagy pathway differentially impacts development and synaptic plasticity. We demonstrate that neuronal activity enhances autophagy activation but diminishes degradative autophagy, thereby driving the pathway towards autophagy-based secretion. Presynaptic knockdown of Snap29, Sec22, or Rab8, proteins implicated in the secretory autophagy pathway, is sufficient to abolish activity-induced synaptic remodeling. This study uncovers secretory autophagy as a transsynaptic signaling mechanism modulating synaptic plasticity.

Drosophila | synaptic remodeling | synaptic plasticity | autophagy | neuromuscular junction

Significance

Neurons are endowed with the capacity to rapidly remodel their synaptic structure and strength in response to varying stimuli. This process, known as activity-induced synaptic remodeling, is crucial for the brain's ability to transform transient experiences into long-term memory. However, signaling mechanisms used by neurons to coordinate the appropriate synaptic changes remain unclear. To this end, we conducted a genetic screen in *Drosophila* against human disease orthologs. We found perturbations in genes associated with neurodegenerative and mental health disorders disproportionately disrupt activity-induced synaptic remodeling compared to synapse development. Furthermore, we found that an autophagy-based release pathway is crucial for activity-induced synaptic remodeling while degradative autophagy maintains synapse development. These findings reveal secretory autophagy as a paradigm regulating synaptic plasticity.

A robust functional neural circuit relies not only on proper synaptic formation and connections during development but also on the ability of the established synapses to rapidly remodel their structure and function in response to varying stimuli (1–3). Such activity-induced synaptic remodeling has been observed in diverse organisms, and shown to be important for behavior, cognition, and learning (2–4). Consequently, defective synaptic plasticity has been linked to numerous neurological disorders (5, 6). Studies have revealed that synaptic development and synaptic plasticity are intertwined (7–9), therefore making it particularly challenging to identify the molecular and cellular pathways required for activity-induced synaptic remodeling without complications from abnormal synapse development.

The *Drosophila* larval neuromuscular junction (NMJ) is as a premier model for investigating mechanisms regulating synaptic plasticity. *Drosophila* is a highly tractable genetic model organism, with approximately 75% of the known disease-causing genes conserved between the fly and human (10). The fly NMJ is a glutamatergic synapse with stereotypical morphology, and shares similar basic molecular, physiological, and neurological properties with mammalian synapses (11, 12). Neuronal activity has been shown to trigger activity-induced synaptic modifications, exemplified in the fly NMJ by the formation of new synaptic boutons, enlargement of existing boutons, and increase in the abundance of postsynaptic glutamate receptors (GluR) (13–16). Various signaling pathways including activation of cyclic adenosine monophosphate (cAMP) signaling, protein kinase A (PKA), bone morphogenic signaling, cell adhesion, and wingless pathways have been shown to regulate activity-dependent new bouton formation at the fly NMJ (13, 14, 16–19); however, aside from the requirement for integrin receptor activation (15), transsynaptic mechanisms responsible for coordinating synaptic remodeling at established synapses (those contributing to bouton enlargement and increase in GluR abundance) remain poorly understood.

In this work, we conducted an RNAi-based genetic screen to identify the molecular pathways important for activity-induced synaptic remodeling. We made the unexpected finding that bifurcation in the macroautophagy pathway (hereafter referred to as autophagy) differentially controls synapse development and synaptic plasticity. Although autophagy is traditionally considered a degradative pathway (20, 21), we show that neuronal activity both activates autophagy and suppresses degradative autophagy,

The authors declare no competing interest.

This article is a PNAS Direct Submission.

[1]Y.-C.C. and Y.G. contributed equally to this work.

[2]Present address: Department of Ophthalmology, University of California San Francisco, San Francisco, CA 94158.

[3]Present address: Neuroscience Graduate Program, University of California San Francisco, San Francisco, CA 94158.

[4]To whom correspondence may be addressed. Email: changkt@usc.edu.

This article contains supporting information online at https://www.pnas.org/lookup/suppl/doi:10.1073/pnas.2315958121/-/DCSupplemental.

Published April 8, 2024.

favoring release through the secretory autophagy pathway. This study reveals that stimulation-induced secretory autophagy represents a mechanism for rapidly coordinating changes across the synapses at the fly NMJ.

Results

An RNAi-Based Genetic Screen to Elucidate Molecular Mechanisms Regulating Activity-Induced Structural Plasticity. To probe molecular pathways regulating structural plasticity, specifically activity-induced increase in bouton size and GluR abundance, we performed an RNAi-based genetic screen in *Drosophila*. We took advantage of the HuDis-TRiP fly RNAi collection, which contains 92% coverage of the highest-confidence fly ortholog of human disease genes (22). Given that altered synaptic plasticity is associated with numerous neurological disorders (5, 6), we focused the screen on genes affecting nervous system functions in humans when mutated. We examined genes that differentially affect 1) synapse development and 2) activity-induced synaptic remodeling using an RNAi-based approach, which allows the uncoupling of the two processes to identify genes most sensitive to perturbation and therefore important for each respective process. We screened through 440 *Drosophila* RNAi lines in the HuDis-TRiP collection available at the Bloomington Stock center, covering 398 unique disease-associated genes in humans (*SI Appendix*, Table S1). To maximize potential for identifying target genes required for activity-induced structural plasticity, RNAi knockdown was performed by crossing to a dual neuronal and muscle driver, *Elav-Gal4; 24B-Gal4*. Both basal synaptic development parameters and activity-induced changes were characterized (Fig. 1*A*). To assay for changes in synaptic development, we analyzed basal synaptic parameters including bouton number per NMJ [bouton number normalized to muscle surface area (MSA)], size of individual type Ib boutons, and intensity of GluR in unstimulated larvae. We categorized a gene as required for normal synaptic development if any of the parameters was abnormal. To study activity-induced synaptic remodeling, we took advantage of the published protocol that a 10-min high K+ stimulation can induce rapid bouton enlargement and increase in postsynaptic GluR abundance similar to electrical stimulation (15). We determined the fold-change in bouton size and GluR intensity following stimulation for each RNAi line, which were normalized to the unstimulated larvae of the same genotype to account for potential differences in basal GluR levels. If the RNAi line failed to display activity-induced increases in either bouton size or GluR abundance, it was classified as a gene required for activity-induced synaptic remodeling. We classified 3 gene groups that influence synaptic morphology when knocked down: Group 1 genes have selective defects in activity-induced synaptic remodeling; Group 2 genes have defects in both synaptic development and activity-induced remodeling; Group 3 genes have defects in synaptic development but not activity-induced remodeling (Fig. 1*B*).

Due to the large number of samples and images generated from the screen, we performed an expedited analysis to assess both basal developmental parameters and activity-induced changes (*Materials and Methods*). We confirmed that this expedited analysis indeed detected activity-induced structural modifications in the driver control at a level comparable to those reported previously (Fig. 1 *C* and *D*), and that the established cutoff parameters successfully detected altered synapse development and activity-induced synaptic modifications in RNAi against shriveled (*shv*), a gene previously shown to regulate both processes (15).

The result of the genetic screen is shown in Fig. 2*A*. All morphological parameters examined showed normal distribution (*SI Appendix*, Fig. S1). There were 71 genes that did not result in any synaptic phenotype and 24 genes that caused lethality when knocked down (*SI Appendix*, Table S2); these were not analyzed further. The majority of the genes showed defects in both synapse development and activity-induced synaptic remodeling (141 genes, Group 2; *SI Appendix*, Table S2). We also uncovered 94 genes that displayed selective defects in activity-induced synaptic remodeling when knocked down (Group 1; *SI Appendix*, Table S2) and 68 genes that disrupted synapse development but not activity-induced synaptic remodeling (Group 3; *SI Appendix*, Table S2). There were some redundant RNAi lines targeting the same human disease gene in the genetic screen. While most overlaps resulted in the same group categorization, a few did not, likely due to the different extent of gene knockdown. These genes were therefore classified by their more severe phenotype, i.e. a Group 1 and wild type result for redundant RNAi lines against the same gene would be classified as Group 1, whereas a Group 1 and Group 2 result for redundant RNAi lines would be classified as Group 2. Interestingly, we never observed disparate classification for a gene in Groups 1 and 3, which are genes specifically affecting acute synaptic remodeling and synapse development, respectively. Together, these results reveal that while synapse development and activity-induced synaptic remodeling could involve overlapping proteins and pathways, it is still possible to uncouple them, as this RNAi knockdown approach identifies key genes most sensitive to alternations.

Mechanisms Regulating Synapse Development and Activity-Induced Synaptic Remodeling. To obtain a broad understanding of the molecular pathways regulating synapse development, we examined all genes that showed altered basal synaptic development parameters (Groups 2 and 3 genes). Kyoto Encyclopedia of Genes and Genomes (KEGG) and Reactome functional enrichment analyses highlight that metabolism pathway, along with lipid, amino acid, and energy metabolism modulate synaptic bouton number (*SI Appendix*, Fig. S2*A*). An enrichment in genes affecting glycosylation and autophagy was also identified. We also examined genes that altered bouton size in unstimulated NMJs when knocked down. Due to the small number of genes uncovered from the screen (11 genes), no functional enrichment was found using KEGG and Reactome analyses, but manual curation identified the presence of three mitochondrial proteins and one peroxisomal proteins, implying that lipid and energy metabolism could be important for the regulation of bouton size. Last, we examined RNAi lines with altered basal GluR levels. We found metabolism, lysosomal function, breakdown of glycosaminoglycan, and glycolysis pathways are important to maintain basal GluR levels (*SI Appendix*, Fig. S2*B*), highlighting that proteostasis and energy metabolism are particularly important.

Next, we aimed to identify key signaling pathways necessary for the rapid, activity-dependent synaptic changes by comparing genes selectively disrupting activity-induced synaptic remodeling (Group 1; *SI Appendix*, Table S2) versus those that affect development (Group 3; *SI Appendix*, Table S2). These two disparate groups allow us to independently examine key proteins affecting synapse development or synaptic plasticity when perturbed. Interestingly, KEGG and Reactome functional pathway analyses revealed that Group 1 showed an enrichment in genes associated with neurodegeneration, as well as autophagy and protein processing in the ER, consistent with an enrichment of ER proteins determined using the GO Cellular Component enrichment analysis (Fig. 2*B*). We also separately examined the functional pathways important for activity-induced bouton size change and GluR abundance. Interestingly, an enrichment in autophagy and GPI-anchor protein

A

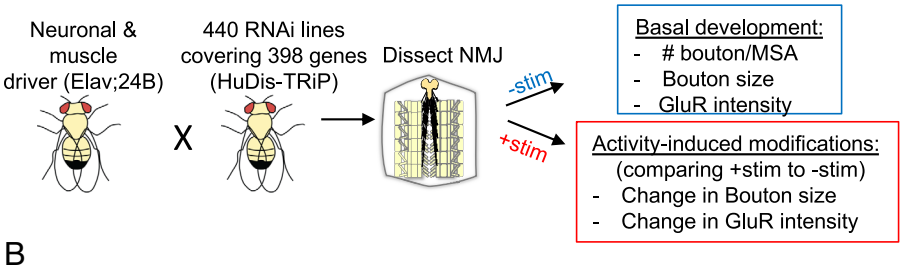

B

	Basal development parameters			Activity-induced structural modifications	
	Bouton #	Bouton size	GluR	Change in bouton size	Change in GluR
Group 1	normal	normal	normal	X	X
Group 2	X	X	X	X	X
Group 3	X	X	X	normal	normal
WT	normal	normal	normal	normal	normal

C

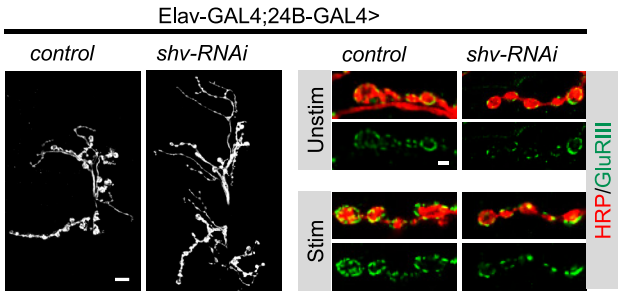

D

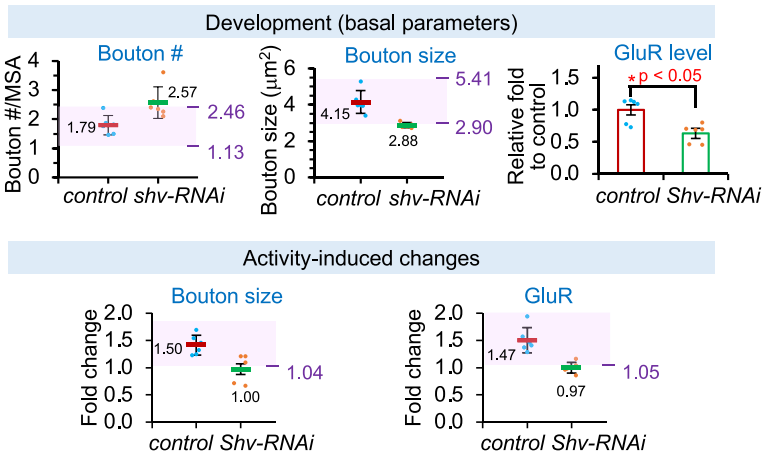

Fig. 1. A RNAi-based genetic screen to identify genes regulating synaptic growth and activity-induced synaptic remodeling. (*A*) Summary of the RNAi-based genetic screen in *Drosophila* using the human disease TRiP (HuDis-TRiP) collection and the morphological parameters examined. (*B*) Group classification used for the genetic screen analysis. (*C*) Representative images of unstimulated (mock) and stimulated synapses at the fly NMJ. Gray-scale images show HRP staining, which outlines the neuronal membrane, revealing a synaptic overgrowth phenotype when *shv* is knocked down using *shv-RNAi* driven by the dual neuronal and muscle *Elav-GAL4;24B-GAL4* driver. (Scale bar, 10 μm.) *Right* images show synaptic boutons stained with HRP (red) and GluRIII antibody (green). (Scale bar, 2 μm.) (*D*) Graphs showing that the cutoff values used in the genetic screen can reliably detect altered synaptic development and activity-induced synaptic remodeling in *shv-RNAi*. Shaded areas highlight cutoff values derived from six driver control NMJs. Bouton number is normalized to MSA, and fold change is calculated by comparing stimulated to mock unstimulated NMJs of the same genotype. Values are mean ± SEM.

synthesis pathways were commonly found for both processes (*SI Appendix*, Fig. S3). Genes selectively disrupting synapse development (Group 3) are highly enriched in lysosomal pathway and amino acid metabolism. GO Cellular Component enrichment analysis also showed a comparable increase in lysosome distribution. We also used the DISEASES database to investigate the relationship between group classification and human diseases. We found that neurological disorders, mental health disorders, intellectual disability, and dementia showed a twofold enrichment in genes affecting activity-induced synaptic remodeling than synapse development (Fig. 2*C* and *SI Appendix*, Fig. S4). Epilepsy and metabolic disorders showed approximately equal distribution, whereas amino acid metabolism disorder and lysosomal storage disease displayed significant enrichment in genes affecting synapse development. These findings reaffirm that structural plasticity is important for cognition and memory.

Role of Autophagy in Activity-Induced Synaptic Remodeling. The finding that autophagy regulates activity-induced synaptic remodeling while lysosomal functions are important for synapse development seemed paradoxical, since canonical autophagy pathway leads to degradation by lysosomes (21). We therefore performed detailed pathway analyses for Groups 1 and 3 genes identified in the KEGG pathway. We found that genes selectively affecting activity-induced synaptic remodeling included those that modulated autophagy activation rather than required for the degradative step of autophagy (Fig. 3*A*; red text). It also contained Snap29, a protein involved in multiple membrane fusion steps including autophagosomes-lysosome fusion and autophagosome fusion with the plasma membrane for release of autophagosomes during secretory autophagy (23–25) (Fig. 3*A*). Conversely, RNAi lines that selectively altered synapse development identified in the screen (Group 3) included 10 different lysosomal degradative

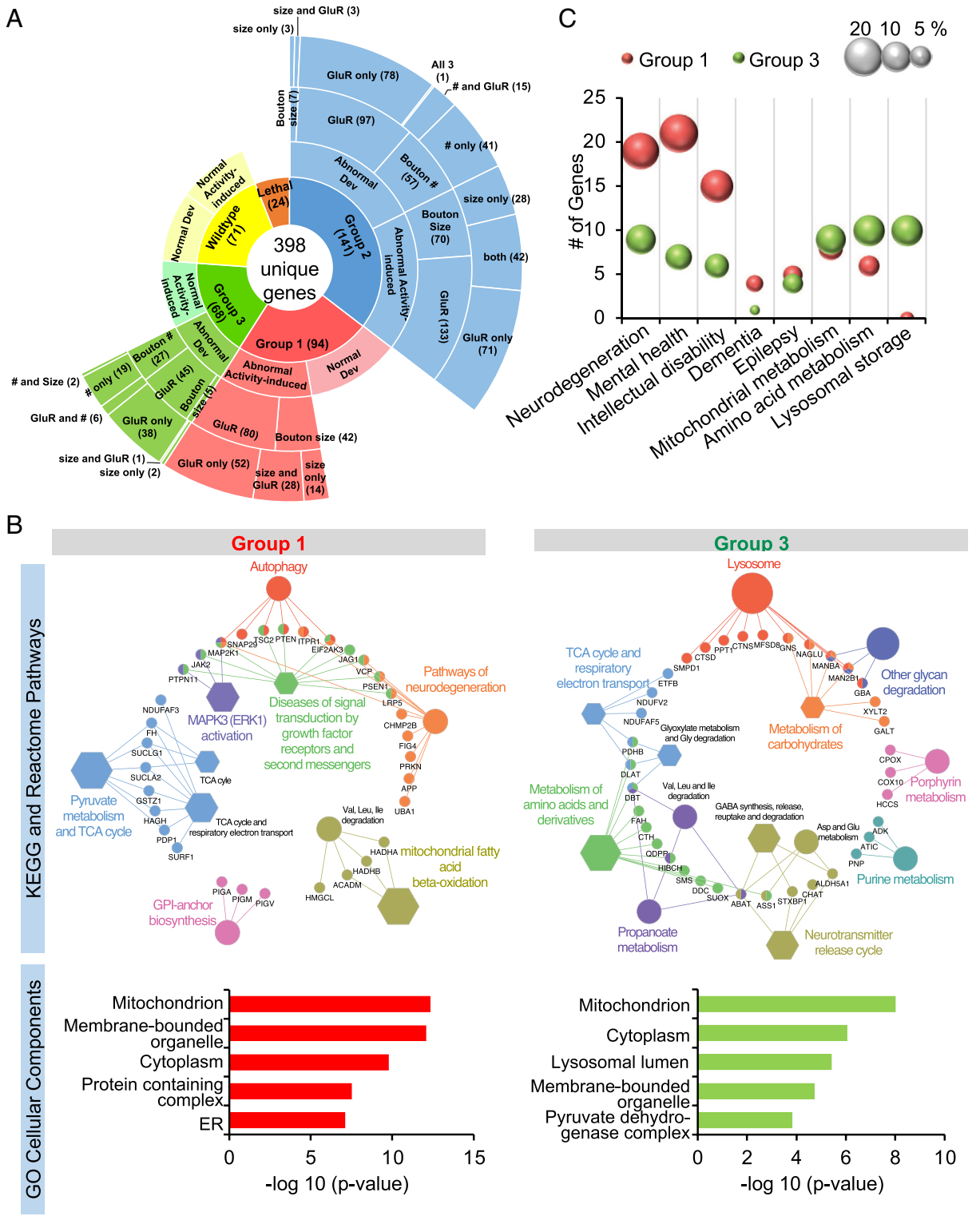

Fig. 2. Bioinformatics analysis of genes selectively perturbing activity-induced synaptic remodeling or synaptic development in the genetic screen. (*A*) Sunburst graph summarizing the results of the genetic screen for 440 RNAi lines against 398 unique human disease orthologs. (*B*) KEGG and Reactome pathway analyses visualized using ClueGo in Cytoscape. Circles represent KEGG pathway and hexagons represent Reactome pathway terms, and larger size represent higher significance. Only term description with *P*-value < 0.05 are shown. Individual nodes (small circles) list the individual genes in the functional pathways. Human gene orthologs were used in bioinformatics analysis. Lower graph shows the GO cellular compartment analysis for Group 1 and 3 genes. (*C*) Graphs show the number of genes identified in the respective disease categories. Size of the sphere indicates percentage of genes in each group belonging to the disease category. Analysis was performed using the DISEASE Database in the String plugin in Cytoscape.

enzymes or lysosomal membrane proteins (green text; Fig. 3*A*), as well as RAB7, a protein important for autophagosome-lysosome fusion and therefore degradative autophagy (26, 27). These findings imply that activity-induced synaptic remodeling does not require degradative autophagy but is most sensitive to disruptions in autophagy-dependent events prior to lysosomal degradation.

To further understand the involvement of autophagy in synaptic plasticity, we first tested the effects of perturbing proteins in the core autophagy machinery, or proteins directly required for

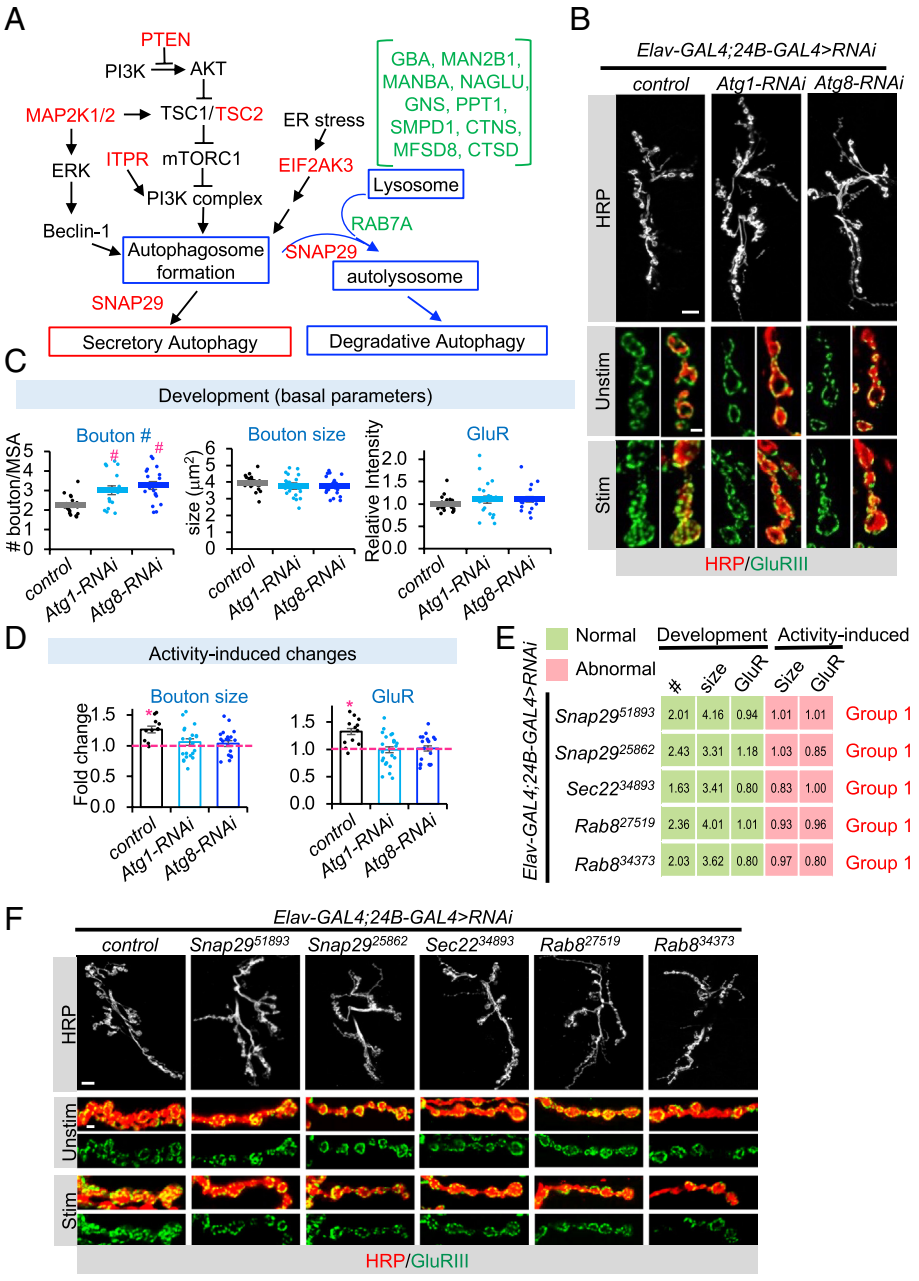

Fig. 3. Bifurcation in autophagy pathway differentially regulates activity-induced synaptic remodeling and synaptic development. (*A*) Autophagy pathway with red text highlighting Group 1 genes and green text highlighting Group 3 genes identified in the genetic screen. Blue outline highlights conventional degradative autophagy pathway. (*B*) Perturbing autophagy core molecular components caused synaptic overgrowth and defective synaptic plasticity. Scale bar, 10 μm for gray-scale images, and 2 μm for colored images. Quantitation of (*C*) basal synaptic development parameters and (*D*) activity-induced synaptic remodeling for the indicated fly lines. Bouton number is normalized to MSA, and fold change is calculated by comparing stimulated to mock unstimulated NMJs of the same genotype. All values are mean ± SEM. One-way ANOVA followed by Tukey's multiple comparison test was used to compare between control and unstimulated samples across genotypes. Student's *t* test was used to compare between unstimulated and stimulated NMJs of the same genotype. $^{\#}P \le 0.05$ when compared to unstimulated control. $^{*}P \le 0.05$ when comparing stimulated to unstimulated NMJs. (*E*) Knockdown of proteins involved in secretory autophagy release pathway in both muscles and neurons selectively blocked activity-induced synaptic remodeling. Same cutoff values from the genetic screen were used for group classification. (*F*) Gray-scale images of unstimulated NMJs labeled with HRP (*Top* row). (Scale bar, 10 μm.) Colored images show unstimulated and stimulated synaptic terminals stained with HRP (red) and GluRIII (green). (Scale bar, 2 μm.)

autophagosome formation. RNAi against autophagy-related proteins atg1 or atg8, which should disrupt both autophagosome formation and subsequent degradative autophagy (28–30), altered synaptic growth, and impaired activity-induced remodeling (Fig. 3 *B*–*D*). These data confirm that autophagy in general is important for both processes and are consistent with our genetic screen results. They also support the idea that bifurcation in the conventional degradative autophagy pathway differentially regulate activity-induced synaptic remodeling and development.

Aside from degradation by lysosomes through the conventional autophagy pathway, autophagosome can also fuse directly with the plasma membrane to release its contents extracellularly through secretory autophagy pathway (31) (Fig. 3*A*). While molecular mechanisms regulating this unconventional secretory autophagy pathway is poorly understood, Snap29, Sec22b, and Rab8a have all been implicated in this pathway by driving autophagosome fusion with the cell membrane for secretion (23, 32–34). Since depletion of Snap29, Sec22, or Rab8 in *Drosophila* is lethal (25, 35, 36), we performed analysis using either available heterozygous mutants or RNAi knockdown driven by the dual neuron and muscle driver. We found $Snap29^{B6\text{-}21}$ heterozygous flies, which showed a 25% decrease in mRNA level (25), displayed defective synaptic remodeling but normal synaptic development (*SI Appendix*, Fig. S5 *A* and *B*), similar to the *Snap29-RNAi* line in the genetic screen (Group 1). The same result was obtained using a second RNAi line against Snap29 ($Snap\text{-}RNAi^{25862}$, Fig. 3 *E* and *F*). Quantitative RT-PCR confirmed that the RNAi lines effectively reduced Snap29 mRNA levels by about 50% (*SI Appendix*, Fig. S5*C*). Next, we examined the effects of disrupting Sec22 and Rab8, which are fly orthologs of human Sec22b and Rab8a, respectively. Sec22b is a SNARE protein that collaborates with Snap29 to regulate secretory autophagy (23, 33), and both Sec22b and Rab8a can facilitate the release of interleukin through secretory autophagy pathway in mammalian cells (23, 32). Quantitative RT-PCR revealed that the *Sec22-RNAi* or *Rab8-RNAi* lines each reduced their respective

mRNA levels by approximately 50% (*SI Appendix*, Fig. S5*C*). This reduction proved sufficient to impair activity-induced bouton size enlargement and GluR increases, while not affecting synaptic development (Fig. 3 *E* and *F*). We also examined the *Rab8* transheterozygous mutant ($Rab8^{1}/Rab8^{B229}$), which was reported to cause synaptic overgrowth (37). Indeed, we found $Rab8^{1}/Rab8^{B229}$ exhibited an increase in bouton number and a decrease in bouton size, but it also failed to undergo activity-induced synaptic remodeling (*SI Appendix*, Fig. S5 *A* and *B*). $Rab8^{1}/Rab8^{B229}$ is a severe mutant with pharate lethality (37), suggesting that extensive depletion of Rab8 also affects development. Collectively, these data reveal that our RNAi knockdown approach can aid the identification of pathways most sensitive to level perturbations, thus avoiding confounding phenotypes caused by maldevelopment. Additionally, they demonstrate that disruptions in the unconventional secretory autophagy pathway prevent acute, activity-induced synaptic changes.

Presynaptic Knockdown of Secretory Autophagy Molecular Machinery Is Sufficient to Block Activity-Induced Synaptic Bouton Enlargement and Increase in GluR Abundance. We speculated that secretory autophagy activation during neuronal activity serves as a paracrine signaling mechanism that allows communication and coordination of synaptic changes across the synapse. To delineate the spatial requirement for secretory autophagy in activity-induced synaptic remodeling, we independently knocked-down Snap29, Rab8, and Sec22 in muscles using *24B-GAL4* or in neurons using *Elav-GAL4* driver. We found that knockdown in muscles resulted in a profound, partial change in synaptic phenotypes (*SI Appendix*, Fig. S6). Specifically, *Rab8-RNAi* expression in muscles could still undergo activity-induced bouton size enlargement, whereas Sec22-RNAi in muscles reduced GluR intensity during development. Sec22 has multiple functional roles including regulation of protein trafficking (38), suggesting that Sec22 may regulate the trafficking of GluR in muscles. We also found that presynaptic knockdown of secretory autophagy molecular components is sufficient to block activity-induced synaptic remodeling (Fig. 4). To further confirm this result, we used the tissue-specific CRISPR approach to knockout *Snap29, Rab8, and Sec22* in neurons (39, 40). Crossing the panneuronally expressed Cas9 (*Elav-Cas9*) to flies expressing CRISPR gRNA for *Snap29*, *Rab8*, or *Sec22* also impaired activity-induced synaptic remodeling (*SI Appendix*, Fig. S7 *A* and *B*). Notably, *Snap29* CRISPR knockout exhibited higher basal GluR level (*SI Appendix*, Fig. S7 *A* and *B*), likely because Snap29 plays dual roles in both secretory autophagy and degradative autophagy pathways (23–25). Given that CRISPR-Cas9-based mutagenesis often causes non-sense-mediated decay of the mutant mRNA (41), we utilized quantitative RT-PCR as a way to confirm the efficacy of the CRISPR approach. Although this method does not directly measure knockout efficiency, the significant reduction in expression indicates successful disruption of Snap29, Sec22, or Rab8 genes using CRISPR (SI Appendix, Fig. S7*C*). Together, these findings suggest that while both muscles and neurons can independently utilize autophagy-based secretory pathway to non-cell autonomously regulate synaptic bouton size and GluR abundance, the communication between the pre- and postsynapse may influence the overall phenotype. Additionally, proteins regulating secretory autophagy may exert different dominant functional roles in distinct cell types. These results also highlight that a significant depletion of a gene in secretory autophagy release pathway can affect synaptic development, particularly when the

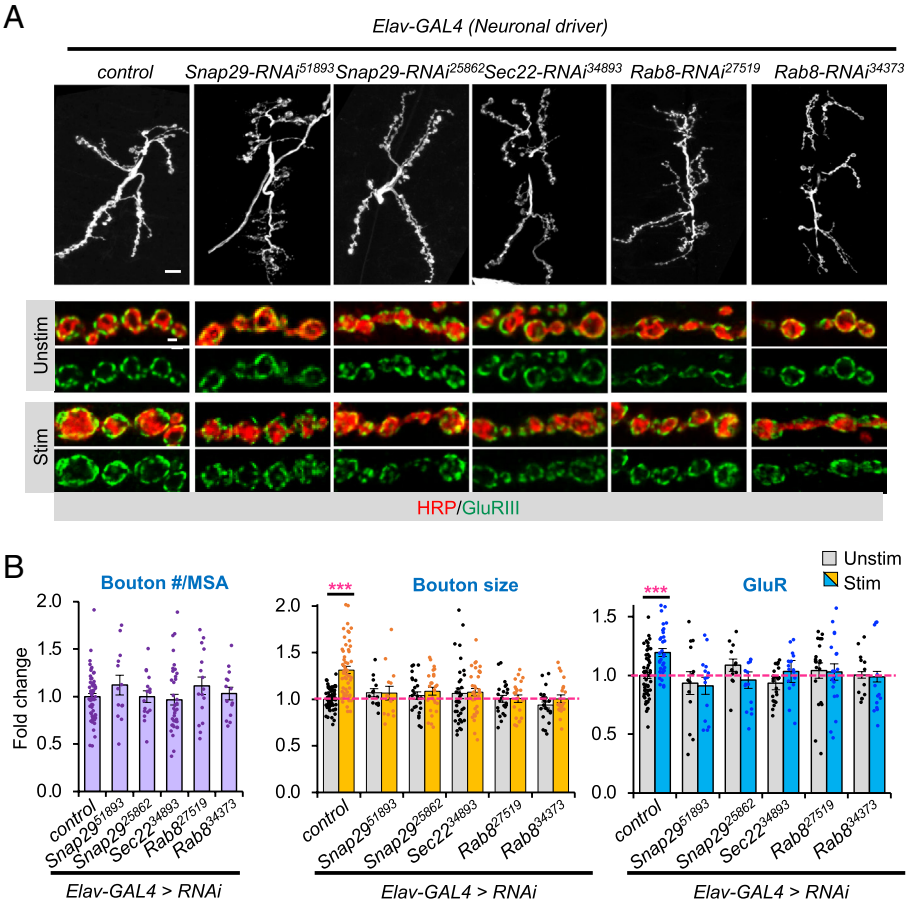

Fig. 4. Neuronal knockdown of secretory autophagy molecular components. (*A*) Gray-scale images of unstimulated NMJs labeled with HRP (*Top* row). (Scale bar, 10 μm.) Colored images show unstimulated and stimulated synaptic terminals stained with HRP (red) and GluRIII (green). (Scale bar, 2 μm.) (*B*) Quantification of fold change in bouton number (normalized to MSA), bouton size, and GluR intensity as indicated. All values are mean ± SEM. Statistics: One-way ANOVA followed by Tukey's multiple comparison test was used to compare between control and unstimulated samples across genotypes. Student's *t* test was used to compare between unstimulated and stimulated NMJs of the same genotype. ***$P \leq 0.001$ when comparing stimulated to unstimulated NMJs.

gene has other cellular functions. Nonetheless, these data indicate that neuronal secretory autophagy pathway is important for promoting activity-induced synaptic remodeling.

Stimulation Blocks Autophagosome-Lysosome Fusion but Enhances Secretory Autophagy. Given that diminishing autophagy-based secretory pathway in neurons is sufficient to block synaptic remodeling, we next set out to monitor autophagy during plasticity-inducing stimulation in neurons. Autophagy is a highly dynamic process that involves autophagosome formation, fusion of autophagosomes with lysosomes to form autolysosomes, and the turnover and removal of autolysosomes (20, 21) (Fig. 5*A*). We monitored total autophagic vesicles using mCherry-atg8a, as the pH-independent nature of mCherry allows labeling of both autophagosomes and autolysosomes (42). Lysosomes were monitored using the marker Lamp1-GFP, and the overlap between mCherry-Atg8a and Lamp1-GFP represented the autolysosomes (42) (Fig. 5*A*). We found that stimulation did not significantly alter the intensity nor the number of mCherry-Atg8a and Lamp1-GFP spots at the NMJ, but it significantly reduced the number of autolysosomes as determined by mCherry-Atg8a and Lamp1-GFP signal colocalization (Fig. 5 *B*–*E* and *SI Appendix*, Fig. S8 *A* and *B*). This stimulation-dependent decrease in autolysosomes could either be due to increased autophagy flux or a block in autophagosome-lysosome fusion. To discern these two cases, we monitored autolysosome number by further depleting autophagosome-lysosome fusion using Rab7-RNAi. We expected that blocking autolysosome formation will exhaust the existing autolysosomes in an activity-dependent manner if enhanced autophagic degradation is the underlying cause. However, Rab7-RNAi showed a similar extent of decrease in the number of autolysosomes poststimulation compared to the control (Fig. 5*C*), revealing that neuronal activity does not enhance autophagy flux but rather inhibits autophagosome-lysosome fusion. Note that Rab7-RNAi also reduced the basal autolysosome number, consistent with its role in mediating autophagosome-lysosome fusion (27). To further validate this result, we visualized the early part of the autophagy pathway using GFP-Atg8a, as the pH-sensitive nature of GFP permits only the labeling of autophagosomes prior to fusion with lysosomes (42). We observed a striking increase in GFP-atg8a intensity and the number of punctate spots following stimulation in control and Rab7-RNAi NMJs (Fig. 5 *F* and *G* and *SI Appendix*, Fig. S8*C*), implying enhanced autophagy activation and consistent with stimulation-induced block in autophagosome-lysosome fusion. Note that we were not able to use the tandemly labeled mCherry-GFP-Atg8a

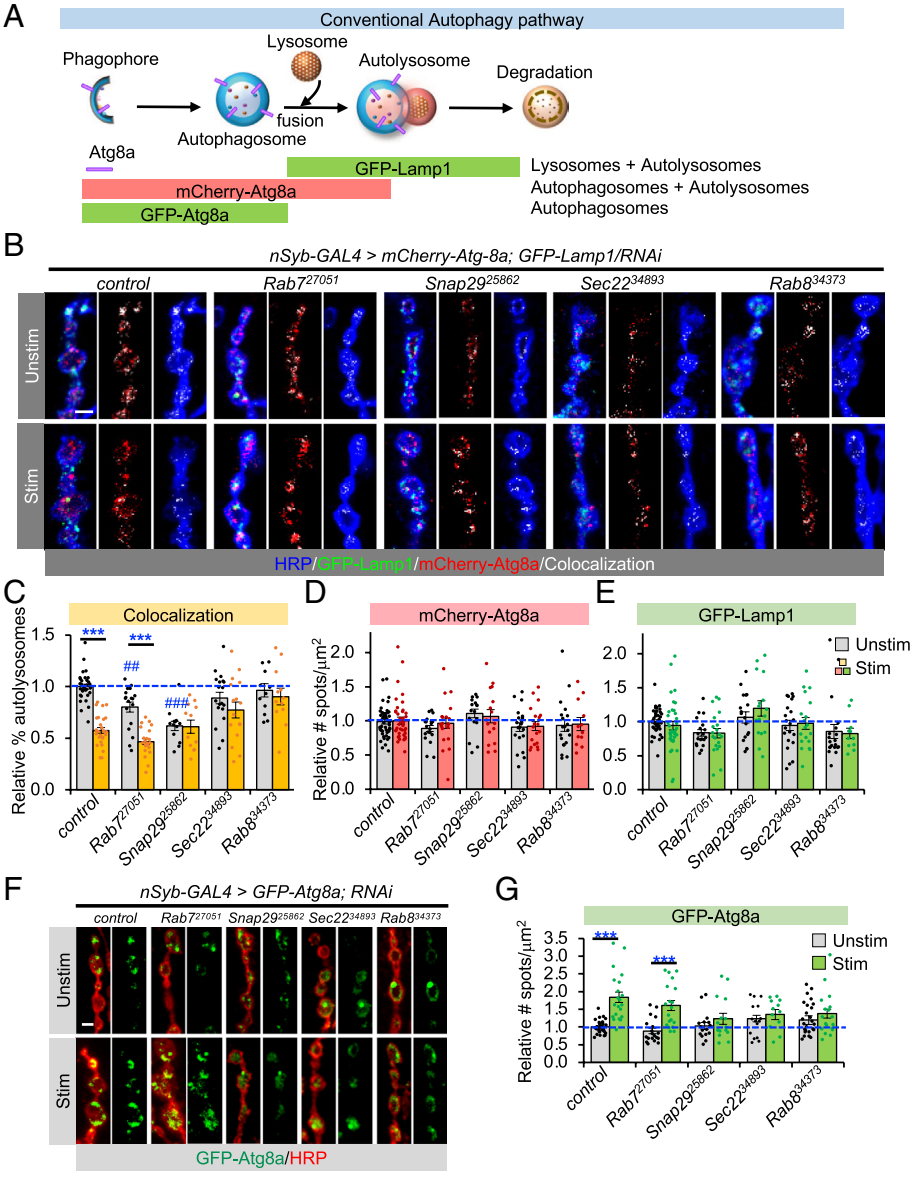

Fig. 5. Stimulation enhances autophagosome formation while inhibiting autophagosome-lysosome fusion. (*A*) Schematic outline of conventional degradative autophagy pathway and fluorescent markers used to detect the different organelles. (*B*) Representative images showing the number of autolysosomes decreased following stimulation. Colocalization between mCherry-Atg8a (red) and GFP-Lamp1 (red) represent the autolysosomes, which are shown in white. HRP (blue) outlines the synaptic bouton membrane. (*C*) Quantification of the fold change in autolysosomes in unstimulated and stimulated NMJs. To account for differences due to the number of autophagic vesicles, the number of autolysosomes was normalized to the number of autophagosomes (mCherry-Atg8a spots) to obtain the percent of autolysosomes in each condition. Fold change is determined by comparing to the mock unstimulated control. (*D*) Fold change in the number of punctate mCherry-Atg8a signal and (*E*) GFP-Lamp1 signal in unstimulated and stimulated NMJs normalized to bouton area. (*F*) Representative images of GFP-Atg8a. Stimulation increased GFP-Atg8a signal, indicating an increase in autophagy initiation. (*G*) Fold change in GFP-Atg8a punctate spots in unstimulated and stimulated NMJs for the indicated genotypes. [Scale bar, 2 μm in (*B*) and (*F*).] All panels show mean ± SEM. Statistics: (*C*) and (*E*) One-way ANOVA followed by Tukey's multiple comparison test was used to compare between control and unstimulated samples across genotypes. Student's *t* test was used to compare between unstimulated and stimulated NMJs of the same genotype. $^{\#\#}P \le 0.01$; $^{\#\#\#}P \le 0.001$ when comparing unstimulated samples of different genotypes to control. $^{***}P \le 0.001$ when comparing stimulated to unstimulated NMJs.

for the above experiments, since this construct did not show sufficient signal to allow detection at the fly NMJ.

Next, we monitored autophagy in Snap29, Sec22, and Rab8-RNAi lines. Knockdown of proteins important for secretory autophagy shunted the pathway toward degradation, since the number of autolysosomes (mCherry-Atg8a and Lamp1-GFP colocalization) no longer declined and autophagosomes (GFP-Atg8a) no longer increased poststimulation (Fig. 5 *B*, *C*, *F*, and *G*). Interestingly, Snap29 also displayed reduced autolysosome signal even without stimulation, consistent with reports that Snap29 also mediates autophagosome-lysosome fusion (24, 25). Together, our results imply that neuronal activity promotes autophagy activation but inhibits autophagosome-lysosome fusion, whereas disrupting autophagy-based secretory pathway drives the pathway toward degradative autophagy pathway.

What is the physiological significance of this stimulation-induced pause in autophagosome-lysosome fusion? We propose that a block in autolysosome formation directs the pathway toward secretory autophagy. Currently there are no known markers for unconventional autophagy-based secretory pathways in neurons. Based on our genetic screen results that knockdown of one of the lysozyme genes, lysozyme P (LysP), resulted in a selective defect in activity-induced synaptic remodeling (*SI Appendix*, Table S2) and a report that lysozyme could be released through secretory autophagy pathways by Paneth cells upon bacterial invasion (36), we explored the possibility that lysozyme is released via this route at the fly NMJ upon stimulation. First, we measured the levels of extracellular lysozyme using a nonpermeabilizing staining condition. Stimulation substantially elevated the presence of extracellular lysozyme at the synapse (Fig. 6*A*). To differentiate the source of extracellular lysozyme, we independently knocked down LysP in neurons or in muscles. Neuronal expression of LysP-RNAi substantially lowered extracellular lysozyme level in unstimulated NMJs while muscle knockdown only mildly suppressed lysozyme level (Fig. 6*B*). Furthermore, neuronal knockdown of LysP abolished the activity-induced increase in extracellular lysozyme signal

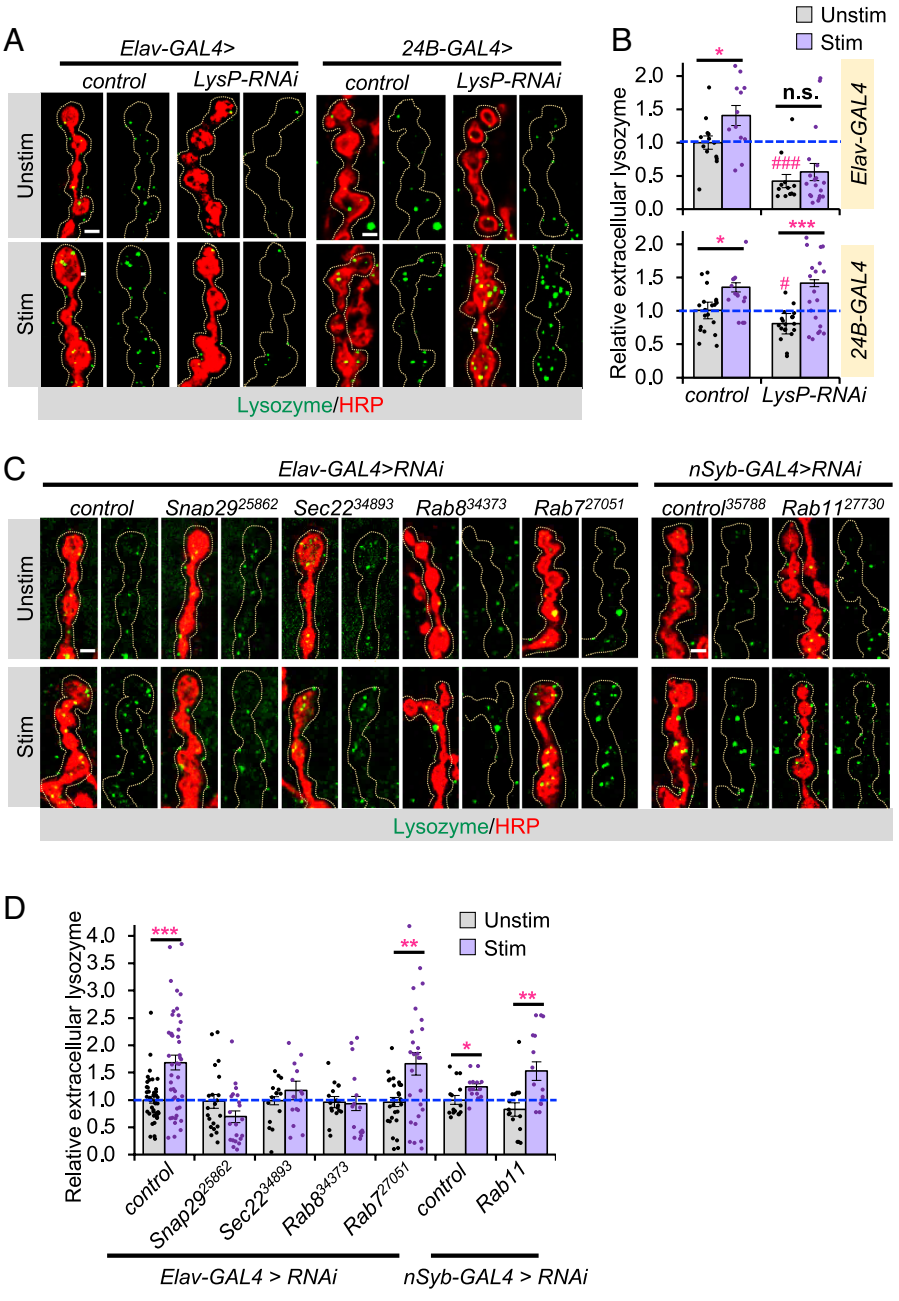

Fig. 6. Activation of secretory autophagy by neuronal activity. (*A*) Extracellular lysozyme staining performed using detergent-free condition. (*B*) Neuronal knockdown of LysP-RNAi diminished activity-induced extracellular lysozyme staining at the synapse while muscle knockdown did not. (Scale bar, 2 μm.) (*C*) Representative images of extracellular lysozyme staining in the RNAi lines as indicated. For (*A*) and (*C*), dashed outline shows the area used to determine extracellular lysozyme level, which is 0.5 μm beyond the neuronal membrane. (Scale bar, 2 μm.) (*D*) Quantification of extracellular synaptic lysozyme staining. Blocking secretory autophagy abolished activity-induced increase in extracellular lysozyme staining. All values are mean ± SEM. Statistics: (*B*) and (*D*) One-way ANOVA followed by Tukey's multiple comparison test was used to compare between control and unstimulated samples across genotypes. Student's *t* test was used to compare between unstimulated and stimulated NMJs of the same genotype. $^{\#}P \le 0.05$; $^{\#\#\#}P \le 0.001$ when comparing unstimulated samples of different genotypes to control. $^{*}P \le 0.05$; $^{**}P \le 0.01$; $^{***}P \le 0.001$ when comparing stimulated to unstimulated NMJs of the same genotype.

at the synapse while muscle knockdown did not (Fig. 6 *A* and *B*). Together, these data indicate that neurons can release lysozymes to the extracellular milieu upon plasticity-inducing stimulation.

To determine whether synaptic lysozyme is released via autophagy-based release pathway, we examined lysozyme release while disrupting proteins involved in secretory autophagy. Neuronal knockdown of Snap29, Rab8, and Sec22 each blocked the activity-induced increase in extracellular lysozyme (Fig. 6 *C* and *D*), suggesting that neuronal activity activates secretory autophagy. We also tested the involvement of the exosome release pathway in lysozyme secretion. To this end, we knocked down the Rab11 GTPase in neurons, which has been shown to modulate endosome recycling and exosome release at the fly NMJ (43). Expression of *Rab11-RNAi* using the Elav-Gal4 driver caused lethality, we thus used another panneuronal driver, *nSyb-GAL4*, which resulted in viable progeny perhaps due to the lower expression level. Neuronal knockdown of Rab11 did not affect stimulation-induced increase in extracellular lysozyme (Fig. 6 *C* and *D*). To ensure that Rab11-RNAi efficiently altered exosome release, we monitored the levels of extracellular neuroglian (Nrg), a protein known to be released in extracellular vesicles through the exosomal pathway (43). Indeed, *Rab11-RNAi* expression in neurons reduced extracellular Nrg levels that were not further elevated by neuronal activity (*SI Appendix*, Fig. S9 *A* and *B*). Conversely, Snap29, Rab8, or Sec22 knockdown displayed normal activity-dependent increase in Nrg, confirming the release of lysozyme and Nrg by independent pathways. We also found that Rab11-RNAi affected both synapse development and activity-induced synaptic remodeling (*SI Appendix*, Fig. S9 *C* and *D*). Interestingly, *Rab7-RNAi*, a protein mediating both autophagosome-lysosome fusion and endolysosomal fusion (44), increased the basal levels of extracellular Nrg (*SI Appendix*, Fig. S9 *A* and *B*), further implying that Nrg may be under homeostatic regulation by lysosomes. Taken together, these data reveal 1) lysozyme can be used to monitor secretory autophagy pathway and is distinct from exosomal release pathway, 2) exosome release pathway can also modulate synapse development and activity-induced synaptic remodeling, and 3) neuronal activity activates secretory autophagy.

Neuronal Knockdown of Secretory Autophagy Components Diminishes Functional Plasticity. To better understand the functional significance of the secretory autophagy pathway, we monitored synaptic transmission using electrophysiology. Neuronal knockdown of secretory autophagy components including Snap29, Rab8, and Sec22 did not alter the amplitude of the miniature excitatory postsynaptic potential (mEPSP) nor evoked EPSP (Fig. 7*A*). Blocking degradative autophagy using *Rab7-RNAi* also yielded normal basal synaptic transmission, consistent with a previous report (45) (Fig. 7*A*). We next investigated posttetanic potentiation (PTP), an activity-dependent plasticity in *Drosophila* that is functionally similar to the initial stages of long-term potentiation in vertebrate central synapses (46). Our previous study showed that PTP is also impaired in a *Drosophila* mutant with activity-induced structural remodeling defects (15). We found that while neuronal knockdown of *Snap29, Sec22, Rab8*, and *Rab7* all diminished synaptic augmentation, only knockdown of secretory autophagy molecular components significantly reduced PTP compared to control (Fig. 7*B*). Collectively, these results suggest

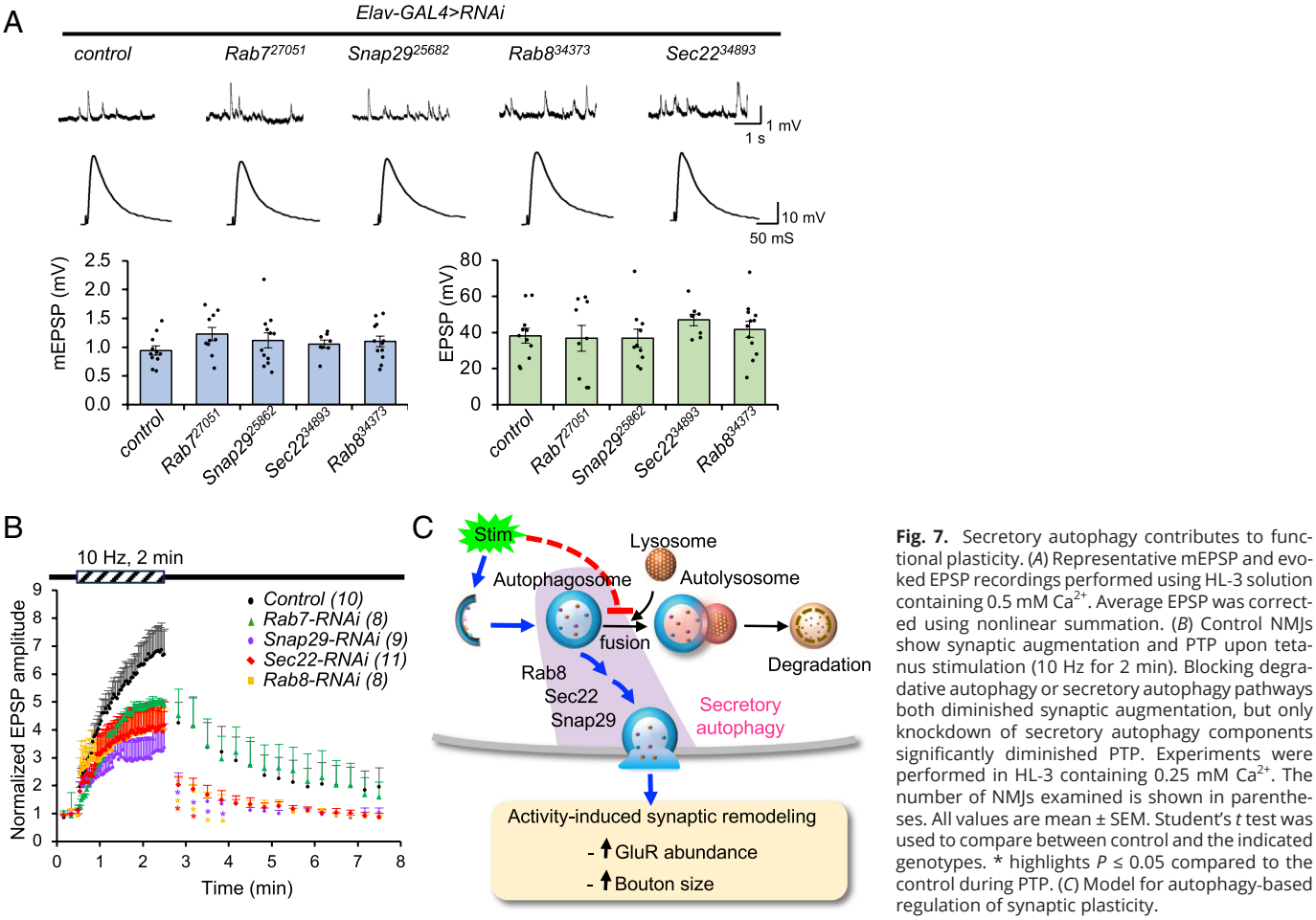

Fig. 7. Secretory autophagy contributes to functional plasticity. (*A*) Representative mEPSP and evoked EPSP recordings performed using HL-3 solution containing 0.5 mM Ca^{2+}. Average EPSP was corrected using nonlinear summation. (*B*) Control NMJs show synaptic augmentation and PTP upon tetanus stimulation (10 Hz for 2 min). Blocking degradative autophagy or secretory autophagy pathways both diminished synaptic augmentation, but only knockdown of secretory autophagy components significantly diminished PTP. Experiments were performed in HL-3 containing 0.25 mM Ca^{2+}. The number of NMJs examined is shown in parentheses. All values are mean ± SEM. Student's *t* test was used to compare between control and the indicated genotypes. * highlights $P \leq 0.05$ compared to the control during PTP. (*C*) Model for autophagy-based regulation of synaptic plasticity.

that autophagy pathway in general is important for synaptic enhancement during neuronal activity, but secretory autophagy release contributes to synaptic strengthening post neuronal activity, underscoring its role in functional synaptic plasticity.

Discussion

Using an RNAi screen against fly orthologs of human disease genes, we found that autophagy-based secretory pathway is a mechanism regulating activity-induced synaptic remodeling at the fly NMJ. While autophagy has previously been linked to synaptic plasticity, it is thought to act through the degradative autophagy pathway to maintain protein homeostasis (47). Our data supports a model in which neuronal activity promotes autophagy activation but dampens autophagosome-lysosome fusion, thereby driving the pathway towards secretory autophagy release. This results in an activity-dependent transsynaptic signal that enables rapid communication and coordination of synaptic changes across the synapse (Fig. 7*C*).

The RNAi genetic screen presented in this paper focused on genes associated with neurological disorders in human. Albeit this is a biased screen, this approach not only allows us to compile information on synaptic changes associated with various diseases of the nervous system, but also to quickly survey candidate genes to identify genes most sensitive to changes in levels and therefore most important for synapse development and synaptic plasticity. Consistent with the idea that synaptic plasticity is important for cognition and memory, we found that intellectual disability, neurodegenerative and mental health disorders are more likely to associate with defects in activity-induced synaptic remodeling than synapse development. We acknowledge that while this RNAi-based approach does not conclusively eliminate the involvement of a gene when the result is negative, it bypasses problems commonly associated with knockout of crucial genes, such as lethality.

Autophagy is classically known as a degradative process in which autophagosomes fuse with lysosomes to breakdown its contents to maintain proteostasis (20, 21). Results showing that knockdown of 10 different lysosomal proteins did not affect activity-induced synaptic remodeling but altered synapse development strongly support that acute, activity-dependent synaptic changes do not rely on degradative autophagy. Aside from the conventional degradative pathway, autophagosomes have recently been shown to be released in response to infection or stress through a processed called secretory autophagy (31). Our data strongly support that neurons utilize secretory autophagy as a mechanism to communicate and coordinate activity-induced synaptic remodeling and maintain synaptic plasticity. First, consistent with reports that neuronal activity induces autophagy activation (48–50), we observed elevated GFP-Atg8a signal poststimulation (Fig. 5 *F* and *G*). Second, knockdown of proteins implicated in secretory autophagy pathway in neurons is sufficient to block activity-induced bouton enlargement and postsynaptic GluR abundance (Fig. 4). Although Snap29, Rab8, or Sec22 each play multiple roles in regulating vesicle trafficking and membrane fusion, they overlap in their ability to facilitate secretory autophagy (23–25, 33, 34, 38). Third, we identified that lysozyme is released through secretory autophagy pathway, and present evidence that neuronal activity enhances lysozyme release (Fig. 6). Lysozyme is typically known as an antimicrobial substance (51), but it also has other less appreciated functions including regulation of bone development and activation of toll-like receptors to mediate neuropathic pain (52, 53). Interestingly, toll-like receptor signaling can modulate multiple processes including neurogenesis and synaptic plasticity (54, 55). Our genetic screen also revealed that knockdown of LysP abolished activity-induced synaptic remodeling. It will be interesting to delineate mechanisms by which lysozyme signaling regulates synaptic plasticity in the future. Note that while we observed an increase in GFP-Atg8a signal consistent with increased autophagy activation during neuronal activity, we did not detect an increase in the number of mCherry-Atg8a spots (which also labels autolysosomes in addition to autophagosomes) as reported previously for prolonged neuronal stimulation (48, 50). This difference is likely due to different stimulation conditions, as a 30-min stimulation was required to elevate mCherry-Atg8a signal (48). This suggests that prolonged stimulation may ultimately activate a different autophagy program to maintain synaptic homeostasis. Future studies examining the signaling cascades regulating autophagy activation during varying neuronal activity will shed light on how neurons utilize different autophagic pathways to optimize function.

How does secretory autophagy lead to bouton enlargement and increase in GluR levels? One potential mechanism is that the fusion of autophagosomes with the plasma membrane through secretory autophagy serves as a means to supply the additional membrane required for bouton enlargement. Simultaneously, the release of signals activates pathways that contribute to further bouton enlargement and an increase in GluR abundance. It is important to note that while this study focused on secretory autophagy as a mechanism regulating activity-induced synaptic remodeling, various cellular events collectively contribute to the complex process of synaptic remodeling. Our bioinformatic analysis also identified a shared requirement for the biosynthesis of GPI-anchored proteins in both bouton enlargement and GluR increase (*SI Appendix*, Fig. S3). As GPI-anchored proteins commonly associate with membrane receptors including adhesion molecules (56), these results imply that signaling through cell surface receptors is crucial for synaptic remodeling. Consistent with this, we had previously identified a requirement for bidirectional integrin signaling in activity-induced synaptic bouton enlargement and increase in GluR (15). Additionally, the genetic screen uncovered an enrichment for genes regulating protein ubiquitination in activity-induced GluR abundance, suggesting that regulation of glutamate receptor turnover and recycling likely plays an important role in this process. In line with this, posttranslational modification through protein ubiquitination has been shown to regulate synaptic plasticity and GluR abundance in various animal models (57–61). Last, it is possible that crosstalk between endosomal and autophagy release pathways also contribute. Aligned with this, we found that knockdown of Rab27A, a protein mediating release of extracellular vesicles downstream of amphisomes (formed by endosome-autophagosome fusion) (62, 63), in our genetic screen as a protein affecting activity-induced remodeling. Rab8a has also been shown to play dual roles in regulating secretory autophagy and extracellular vesicle release downstream of endosome-autophagosome pathway (63). Thus, future investigations examining protein ubiquitination, as well as crosstalk between endosome, autophagosome, and lysosome pathways will provide insights into how neurons integrate various cellular pathways to coordinate activity-dependent synaptic changes. Identification of cargos released through autophagy-based secretion will also facilitate our understandings of the physiological significance of this signaling pathway and its role in neurodegenerative disorders.

Materials and Methods

Drosophila Culture and Stocks. Flies were grown on standard cornmeal, yeast, sugar, and agar medium at 25 °C under a 12 h dark/light cycle. Strains used are detailed in *SI Appendix*, *SI Materials and Methods*, and TRiP RNAi lines used in the genetic screen are listed in *SI Appendix*, Table S1.

Dissection and Stimulation. NMJ dissection and stimulation were performed as described (15) and as detailed in *SI Appendix, SI Materials and Methods*.

Immunocytochemistry. Immunostaining protocols and antibodies used are described in *SI Appendix, SI Materials and Methods*.

Imaging. Images of synaptic boutons from muscle 6/7, A2 or A3 were acquired using either a Zeiss LSM800 or Olympus FV3000 confocal microscope. To expedite image capture for the genetic screen, 3-z stacks at 2 μm interval were used to capture the entire depth of the synaptic boutons at 40x (Zeiss) or 4-z stacks at 1.5 μm interval were captured using Olympus at 60×. A single plane 10× image was also taken for each animal in order to determine the MSA. To establish changes in basal GluR level, unstimulated, mock control larvae were always dissected and imaged in parallel with test genotypes for each experiment. Stimulated and unstimulated animals per genotype were also performed and imaged in parallel using the same conditions in order to measure fold-change in bouton size and GluR intensity. A minimum of 5 NMJs from a minimum of two larvae were imaged per condition and per genotype for the genetic screen. For all other experiments, images were acquired using an Olympus FV3000 confocal microscope at 60× with 1.6 zoom.

Image Analysis. For the genetic screen, an expedited analysis using 15 type Ib boutons belonging to a minimum of two branches of axons at muscles 6/7 were manually circled in Image J to determine the average bouton size and average GluR intensity. Control NMJ (w1118 crossed to driver control) was used to establish the cutoff parameters. For morphological parameters that could be quantified by absolute values such as bouton number and size, and the fold-change in bouton size and GluR intensity following stimulation (normalized to unstimulated NMJ of the same genotype), a value that is 2 SDs (95% confidence) away from the mean was defined as abnormal. For basal GluR level in unstimulated RNAi lines, GluR intensity was compared to control NMJs dissected in parallel, and a P-value < 0.05 compared to control was defined as abnormal. For subsequent validation experiments involving key RNAi lines, all Type Ib boutons at the synapse were analyzed. To determine extracellular/secreted lysozyme or neuroglian level, individual synaptic boutons were circled at 0.5 μm beyond HRP staining. Average staining intensity (normalized to bouton area) was always compared to mock controls done within the same experimental set to obtain fold change. Additional details on quantification of GFP-Atg8a, mCherry-Atg8a, and GFP-Lamp1 puncta are detailed in *SI Appendix, SI Materials and Methods*.

Quantitative RT-PCR. RNA extraction and primer information are detailed in *SI Appendix, SI Materials and Methods*.

KEGG Pathway, Reactome Pathway, and DISEASE Analyses. Cytoscape was used to display functional pathway analysis results. The String database plugin was used to retrieve functional enrichment for Gene Ontology terms including cellular component analysis and DISEASE database analysis. Human gene orthologs were used in bioinformatics analysis. KEGG and Reactome analyses were performed using ClueGO plugin in Cytoscape. A minimum of 3 genes in each GO term and a $P < 0.05$ were used as criteria.

Electrophysiology. NMJ dissection and electrophysiology recordings were done as described (15) and detailed in *SI Appendix, SI Materials and Methods*.

Statistical Analysis. All data are presented as mean ± SEM. Sample numbers are shown in the graphs or figure legends and represent biological replicates. The number of samples used is consistent with established standards in the literature. Samples were randomized during dissection, image collection, and data analyses to minimize bias. To compare unstimulated and stimulated samples of the same genotype, Student's t test was used. For multiple samples, One-way ANOVA followed by post hoc analysis with Turkey's multiple comparison test and was used to determine statistical significance.

Data, Materials, and Software Availability. All study data are included in the article and/or supporting information.

ACKNOWLEDGMENTS. We would like to thank all the undergraduate students in the lab over the years for their help with the genetic screen, and members of the lab for their helpful comments and critical reading of the manuscript. K.T.C. is supported by NIH grants R01NS080946 and R01NS102260.

Author affiliations: [a]Zilkha Neurogenetic Institute, Keck School of Medicine, University of Southern California, Los Angeles, CA 90033; and [b]Department of Physiology and Neuroscience, Keck School of Medicine, University of Southern California, Los Angeles, CA 90033

Author contributions: J.Y.L. and K.T.C. designed research; Y.-C.C., Y.G., J.Y.L., Y.-J.P., and J.L. performed research; Y.-C.C., Y.G., J.Y.L., Y.-J.P., J.L., and K.T.C. analyzed data; and Y.-C.C., Y.G., and K.T.C. wrote the paper.

1. R. Lamprecht, J. LeDoux, Structural plasticity and memory. *Nat. Rev. Neurosci.* **5**, 45–54 (2004).
2. A. Citri, R. C. Malenka, Synaptic plasticity: Multiple forms, functions, and mechanisms. *Neuropsychopharmacology* **33**, 18–41 (2008).
3. P. Caroni, F. Donato, D. Muller, Structural plasticity upon learning: Regulation and functions. *Nat. Rev. Neurosci.* **13**, 478–490 (2012).
4. C. H. Bailey, E. R. Kandel, K. M. Harris, Structural components of synaptic plasticity and memory consolidation. *Cold Spring Harb. Perspect. Biol.* **7**, a021758 (2015).
5. T. V. Bliss, G. L. Collingridge, R. G. Morris, Synaptic plasticity in health and disease: Introduction and overview. *Philos. Trans. R. Soc. Lond. B Biol. Sci.* **369**, 20130129 (2014).
6. L. G. Appelbaum, M. A. Shenasa, L. Stolz, Z. Daskalakis, Synaptic plasticity and mental health: Methods, challenges and opportunities. *Neuropsychopharmacology* **48**, 113–120 (2023).
7. C. Lohmann, H. W. Kessels, The developmental stages of synaptic plasticity. *J. Physiol.* **592**, 13–31 (2014).
8. K. Shen, C. W. Cowan, Guidance molecules in synapse formation and plasticity. *Cold Spring Harb. Perspect. Biol.* **2**, a001842 (2010).
9. D. Kilinc, The emerging role of mechanics in synapse formation and plasticity. *Front. Cell Neurosci.* **12**, 483 (2018).
10. L. T. Reiter, L. Potocki, S. Chien, M. Gribskov, E. Bier, A systematic analysis of human disease-associated gene sequences in Drosophila melanogaster. *Genome Res.* **11**, 1114–1125 (2001).
11. H. Keshishian, K. Broadie, A. Chiba, M. Bate, The drosophila neuromuscular junction: A model system for studying synaptic development and function. *Annu. Rev. Neurosci.* **19**, 545–575 (1996).
12. C. A. Collins, A. DiAntonio, Synaptic development: Insights from Drosophila. *Curr. Opin. Neurobiol.* **17**, 35–42 (2007).
13. B. Ataman *et al.*, Rapid activity-dependent modifications in synaptic structure and function require bidirectional Wnt signaling. *Neuron* **57**, 705–718 (2008).
14. A. Vasin *et al.*, Synapsin regulates activity-dependent outgrowth of synaptic boutons at the Drosophila neuromuscular junction. *J. Neurosci.* **34**, 10554–10563 (2014).
15. J. Y. Lee, J. Geng, J. Lee, A. R. Wang, K. T. Chang, Activity-induced synaptic structural modifications by an activator of integrin signaling at the *Drosophila* neuromuscular junction. *J. Neurosci.* **37**, 3246–3263 (2017).
16. P. I. Tsai *et al.*, Activity-dependent retrograde laminin A signaling regulates synapse growth at Drosophila neuromuscular junctions. *Proc. Natl. Acad. Sci. U.S.A.* **109**, 17699–17704 (2012).
17. B. Berke, J. Wittnam, E. McNeill, D. L. Van Vactor, H. Keshishian, Retrograde BMP signaling at the synapse: A permissive signal for synapse maturation and activity-dependent plasticity. *J. Neurosci.* **33**, 17937–17950 (2013).
18. Z. D. Piccioli, J. T. Littleton, Retrograde BMP signaling modulates rapid activity-dependent synaptic growth via presynaptic LIM kinase regulation of cofilin. *J. Neurosci.* **34**, 4371–4381 (2014).
19. R. W. Cho *et al.*, Phosphorylation of complexin by PKA regulates activity-dependent spontaneous neurotransmitter release and structural synaptic plasticity. *Neuron* **88**, 749–761 (2015).
20. A. Fleming *et al.*, The different autophagy degradation pathways and neurodegeneration. *Neuron* **110**, 935–966 (2022).
21. D. J. Klionsky, S. D. Emr, Autophagy as a regulated pathway of cellular degradation. *Science* **290**, 1717–1721 (2000).
22. Y. Hu *et al.*, FlyRNAi.org-the database of the Drosophila RNAi screening center and transgenic RNAi project: 2021 update. *Nucleic Acids Res.* **49**, D908–D915 (2021).
23. T. Kimura *et al.*, Dedicated SNAREs and specialized TRIM cargo receptors mediate secretory autophagy. *EMBO J.* **36**, 42–60 (2017).
24. E. Itakura, C. Kishi-Itakura, N. Mizushima, The hairpin-type tail-anchored SNARE syntaxin 17 targets to autophagosomes for fusion with endosomes/lysosomes. *Cell* **151**, 1256–1269 (2012).
25. E. Morelli *et al.*, Multiple functions of the SNARE protein Snap29 in autophagy, endocytic, and exocytic trafficking during epithelial formation in Drosophila. *Autophagy* **10**, 2251–2268 (2014).
26. N. Fujita *et al.*, Genetic screen in Drosophila muscle identifies autophagy-mediated T-tubule remodeling and a Rab2 role in autophagy. *Elife* **6**, e23367 (2017).
27. S. Jäger *et al.*, Role for Rab7 in maturation of late autophagic vacuoles. *J. Cell Sci.* **117**, 4837–4848 (2004).
28. N. N. Noda, Y. Fujioka, Atg1 family kinases in autophagy initiation. *Cell Mol. Life Sci.* **72**, 3083–3096 (2015).
29. Z. Xie, U. Nair, D. J. Klionsky, Atg8 controls phagophore expansion during autophagosome formation. *Mol. Biol. Cell* **19**, 3290–3298 (2008).
30. Z. Xie, D. J. Klionsky, Autophagosome formation: Core machinery and adaptations. *Nat. Cell Biol.* **9**, 1102–1109 (2007).
31. C. D. Gonzalez, R. Resnik, M. I. Vaccaro, Secretory autophagy and its relevance in metabolic and degenerative disease. *Front. Endocrinol. (Lausanne)* **11**, 266 (2020).
32. N. Dupont *et al.*, Autophagy-based unconventional secretory pathway for extracellular delivery of IL-1β. *EMBO J.* **30**, 4701–4711 (2011).
33. S. Martinelli *et al.*, Stress-primed secretory autophagy promotes extracellular BDNF maturation by enhancing MMP9 secretion. *Nat. Commun.* **12**, 4643 (2021).
34. J. New, S. M. Thomas, Autophagy-dependent secretion: Mechanism, factors secreted, and disease implications. *Autophagy* **15**, 1682–1693 (2019).

35. X. Zhao *et al.*, Sec22 regulates endoplasmic reticulum morphology but not autophagy and is required for eye development in Drosophila. *J. Biol. Chem.* **290**, 7943–7951 (2015).
36. S. Bel *et al.*, Paneth cells secrete lysozyme via secretory autophagy during bacterial infection of the intestine. *Science* **357**, 1047–1052 (2017).
37. R. J. West, Y. Lu, B. Marie, F. B. Gao, S. T. Sweeney, Rab8, POSH, and TAK1 regulate synaptic growth in a Drosophila model of frontotemporal dementia. *J. Cell Biol.* **208**, 931–947 (2015).
38. W. Sun, B. X. Tian, S. H. Wang, P. J. Liu, Y. C. Wang, The function of SEC22B and its role in human diseases. *Cytoskeleton (Hoboken)* **77**, 303–312 (2020).
39. H. Meltzer *et al.*, Tissue-specific (ts)CRISPR as an efficient strategy for in vivo screening in Drosophila. *Nat. Commun.* **10**, 2113 (2019).
40. G. T. Koreman *et al.*, Upgraded CRISPR/Cas9 tools for tissue-specific mutagenesis in Drosophila. *Proc. Natl. Acad. Sci. U.S.A.* **118**, e2014255118 (2021).
41. R. Tuladhar *et al.*, CRISPR-Cas9-based mutagenesis frequently provokes on-target mRNA misregulation. *Nat. Commun.* **10**, 4056 (2019).
42. C. Mauvezin, C. Ayala, C. R. Braden, J. Kim, T. P. Neufeld, Assays to monitor autophagy in Drosophila. *Methods* **68**, 134–139 (2014).
43. R. B. Walsh *et al.*, Opposing functions for retromer and Rab11 in extracellular vesicle traffic at presynaptic terminals. *J. Cell Biol.* **220**, e202012034 (2021).
44. T. Wang, Z. Ming, W. Xiaochun, W. Hong, Rab7: Role of its protein interaction cascades in endo-lysosomal traffic. *Cell Signal.* **23**, 516–521 (2011).
45. S. Cherry *et al.*, Charcot-Marie-Tooth 2B mutations in rab7 cause dosage-dependent neurodegeneration due to partial loss of function. *Elife* **2**, e01064 (2013).
46. D. E. Featherstone, K. Broadie, Surprises from Drosophila: Genetic mechanisms of synaptic development and plasticity. *Brain Res. Bull.* **53**, 501–511 (2000).
47. J. Y. Hwang, J. Yan, R. S. Zukin, Autophagy and synaptic plasticity: Epigenetic regulation. *Curr. Opin. Neurobiol.* **59**, 207–212 (2019).
48. S. F. Soukup *et al.*, A LRRK2-dependent EndophilinA phosphoswitch is critical for macroautophagy at presynaptic terminals. *Neuron* **92**, 829–844 (2016).
49. S. Yang *et al.*, Presynaptic autophagy is coupled to the synaptic vesicle cycle via ATG-9. *Neuron* **110**, 824–840.e10 (2022).
50. A. T. Bademosi *et al.*, EndophilinA-dependent coupling between activity-induced calcium influx and synaptic autophagy is disrupted by a Parkinson-risk mutation. *Neuron* **111**, 1402–1422.e13 (2023).
51. S. A. Ragland, A. K. Criss, From bacterial killing to immune modulation: Recent insights into the functions of lysozyme. *PLoS Pathog.* **13**, e1006512 (2017).
52. T. J. Hilliard, G. Meadows, A. J. Kahn, Lysozyme synthesis in osteoclasts. *J. Bone Miner. Res.* **5**, 1217–1222 (1990).
53. S. Yadav, A. Surolia, Lysozyme elicits pain during nerve injury by neuronal Toll-like receptor 4 activation and has therapeutic potential in neuropathic pain. *Sci. Transl. Med.* **11**, eaav4176 (2019).
54. E. Okun, K. J. Griffioen, M. P. Mattson, Toll-like receptor signaling in neural plasticity and disease. *Trends Neurosci.* **34**, 269–281 (2011).
55. K. J. Seong *et al.*, Toll-like receptor 5 promotes the neurogenesis from embryonic stem cells and adult hippocampal neural stem cells in mice. *Stem Cells* **40**, 303–317 (2022).
56. J. W. Um, J. Ko, Neural glycosylphosphatidylinositol-anchored proteins in synaptic specification. *Trends Cell Biol.* **27**, 931–945 (2017).
57. M. Burbea, L. Dreier, J. S. Dittman, M. E. Grunwald, J. M. Kaplan, Ubiquitin and AP180 regulate the abundance of GLR-1 glutamate receptors at postsynaptic elements in C. elegans. *Neuron* **35**, 107–120 (2002).
58. L. A. Schwarz, B. J. Hall, G. N. Patrick, Activity-dependent ubiquitination of GluA1 mediates a distinct AMPA receptor endocytosis and sorting pathway. *J. Neurosci.* **30**, 16718–16729 (2010).
59. A. K. Fu *et al.*, APC(Cdh1) mediates EphA4-dependent downregulation of AMPA receptors in homeostatic plasticity. *Nat. Neurosci.* **14**, 181–189 (2011).
60. J. Widagdo *et al.*, Activity-dependent ubiquitination of GluA1 and GluA2 regulates AMPA receptor intracellular sorting and degradation. *Cell Rep.* **10**, 783–795 (2015).
61. K. F. Haas, S. L. Miller, D. B. Friedman, K. Broadie, The ubiquitin-proteasome system postsynaptically regulates glutamatergic synaptic function. *Mol. Cell Neurosci.* **35**, 64–75 (2007).
62. M. Ostrowski *et al.*, Rab27a and Rab27b control different steps of the exosome secretion pathway. *Nat. Cell Biol.* **12**, 19–30; suppl. pp. 11–13 (2010).
63. Y. D. Chen *et al.*, Exophagy of annexin A2 via RAB11, RAB8A and RAB27A in IFN-γ-stimulated lung epithelial cells. *Sci. Rep.* **7**, 5676 (2017).